Final version published as: Boparai, M., Oberc, C., & Li, P. C. H. (2021). Presence of an EML4-ALK gene fusion detected by microfluidic chip DNA hybridization. Bioscience, Biotechnology, and Biochemistry, zbaa043. https://doi.org/10.1093/bbb/zbaa043.

Presence of an EML4-ALK gene fusion detected by microfluidic chip DNA hybridization

Montek Boparai*, Christopher Oberc*, Paul C.H. Li*,

**Department of Chemistry, Simon Fraser University, 8888 University Drive, BC, Canada, V5A 1S6*

Corresponding author: Paul C.H. Li, paulli@sfu.ca
Tel: 778-782-5956
Fax: 778-782-3765

Abstract

Non-small cell lung cancer (NSCLC) accounts for ~80-85% of all lung cancer cases, and the EML4-ALK fusion oncogene is a well-known contributor to NSCLC cases. Expensive methods such as FISH, IHC, and NGS have previously been used to detect the EML4-ALK fusion oncogene. Here, a cost-effective and facile method of detecting and differentiating an EML4-ALK fusion oncogene from the wildtype gene has been accomplished by hybridization using the microfluidic biochip. First, oligonucleotide probes were confirmed for successful detection of immobilized sense strands. Second, capture of the sense PCR product strands (fusion and WT) and their subsequent detection and differentiation were accomplished. Our proof-of-concept study shows the ability to detect 1% fusion products, among WT ones.

Key words: Microfluidic chip, lung cancer, DNA hybridization, oligonucleotide immobilization, fluorescence detection

Introduction

Non-small cell lung cancer (NSCLC) accounts for ~80-85% of all lung cancer cases (1, 2). One genetic mutation among the NSCLC cases is caused by the fusion of the EML4 gene and the ALK gene (3). Both the genes of EML4 (echinoderm microtubule-associated protein-like 4) and ALK (anaplastic lymphoma kinase) are located on chromosome 2, separated by ~12 megabases, and the fusion of these genes occurs to produce the EML4-ALK fusion oncogene (4). The expression of this fusion gene results in uncontrolled cell proliferation (5, 6).

There are many variants of the EML4-ALK fusion oncogene with the differences in the site of fusion (7). The most prevalent mutation is variant 1 (7-9), in which the fusion occurs between exon 20 of ALK and EML4 exon 13 (10).

Detection of the EML4-ALK gene fusion has been achieved by using techniques such as real time polymerase chain reaction (RT-PCR) (7, 11, 12), DNA microarrays (13-15), fluorescence in situ hybridization (FISH) (16-18), immunohistochemistry (IHC) (16-18), or next-generation sequencing (NGS) (16, 18, 19), which are expensive methods. In this proof-of-concept study, a microfluidic biochip is used in which DNA hybridization occurs to allow for the cost-effective detection of the wildtype and fusion gene sequences in a sample. The biochip contains microchannels through which microliters of sample solutions can be injected for hybridization with the immobilized components on the biochip surface, and this method has previously been used to detect KRAS mutations (20, 21). By using the biochip made in the lab, we have greater control over the target sequences and the probes which are to be used for hybridization.

Therefore, the use of the biochip hybridization method requires low sample consumption (i.e. nanograms of samples) and flexible choice of probes, which makes this a cost-efficient method.

Materials and Methods

There were no human or animal subjects used in this study.

Microfluidic biochip Formation

The 16-microchannel biochip consists of a polydimethylsiloxane (PDMS) slab and a functionalized glass slide (***Fig. 1***). The PDMS slab was synthesized in the lab by mixing the elastomer with a curing agent, then pouring the solution onto a mold and allowing it to cure at 22°C (22). After removal of the slab from the mold, holes were punched into the slab at the ends of the sixteen trenches. The slab was then reversibly sealed onto a functionalized glass slide so that trenches became microchannels and holes became wells. Afterwards, solutions were injected on the wells for introduction into the microchannels and allowed to react with the glass slide surface (***Fig. 1***).

Glass Slide Functionalization

A 75 mm x 50 mm glass slide was first cleaned with 100 mL of Piranha solution consisting of 70 mL of 98% H_2SO_4 and 30 mL of 30% H_2O_2 for 15 min. After drying, the slide was treated with a (3-aminopropyl)triethoxysilane (APTES) solution containing 2 mL APTES and 98 mL ethanol (95%) for 20 min. This reaction was conducted under an inert N_2 atmosphere and was followed

by heating the slide at 120°C for 1 h. The slide was then reacted with a 100 mL 5% glutaraldehyde solution in 1x phosphate-buffered saline (PBS) for 1 h.

DNA Oligomer Sequences

The EML4-ALK fusion and the wildtype ALK sequence were cross-referenced with the National Center for Biotechnology Information (NCBI) and the European Nucleotide Archive (ENA) databases to ensure sequence accuracy. Target strands and detection probes were ordered from Integrated DNA Technologies (IDT). Oligonucleotide probes were designed, and they were either complementary to the EML4 portion of the gene fusion (EML4 probe) or complementary to the ALK portion (ALK probes 1 and 2), and they were biotin-labelled on their 5' ends for detection. An 85-mer target sequence (fusion oligomer) was designed encompassing the site of the EML4-ALK fusion such that it contained both the EML4 and ALK portions of the fusion allowing it to bind to both the EML4 and ALK probes. A 55-mer target (WT oligomer) was designed consisting of the wildtype ALK sequence such that the WT probe would hybridize but the EML4 probe would not.

Two oligomers (gBlock gene fragments) were obtained to serve as double-stranded templates for producing PCR products for the fusion and wild-type ALK sequences. Two forward primers were designed to amplify the fusion sequence and the wildtype sequence; the same reverse primer was used to amplify the two sequences, since the 3' end of both sequences consists of the same ALK wildtype portion. The sense strand of the PCR products would be immobilized on the glass slide using the complementary sequence of the forward primer as the capture strand; the 3'

amino labelled capture strands (antisense) were designed in order to stick out the target strand away from the slide surface.

Analysis of T_m and hairpin for the target strands, primers and probes was achieved using software such as MFOLD, IDT and New England Biolabs (NEB) T_m calculators to ensure optimal hybridization thermodynamics (23-27).

Amplification of fusion and wildtype sequences

PCR buffer and Taq DNA polymerase were obtained from Applied Biological Materials Inc. (Richmond, BC, Canada) and dNTP's from Thermo Scientific Inc. (Waltham, MA, USA). PCR was performed in a 50 µL reaction volume and reagent concentrations were 1X PCR Buffer, 200 µM of each nucleotide (dATP, dGTP, dCTP, dTTP), 300 nM each of forward and reverse primers if symmetric PCR products were desired or 450 nM and 150 nM of forward and reverse primers, respectively, if asymmetric PCR products were desired, 10 ng DNA template (either fusion or wildtype), and 5U Taq DNA polymerase. PCR was performed using the ^{3}Prime thermocycler (Techne). Thermal cycling parameters started with a 3 min 94°C initial denaturation followed by 30 cycles of 95 °C (denaturation), 50 °C (annealing), and 72 °C (elongation) each for 30 s. PCR amplified products were purified using a PCR purification kit (Qiagen). Following purification, the ratios of DNA absorbances at specific wavelengths (nm), i.e. 260/230 ratio and 260/280 ratio, were obtained using the Nanodrop spectrometer analysis. If the 260/230 ratio was close to 2-2.22 and the 260/280 ratio was close to 1.8, the products were deemed pure and were used in subsequent experiments. The symmetric PCR products were diluted to 22 ng/µL in hybridization buffer, and the the fusion and wildtype asymmetric PCR products were diluted to 19.6 ng/µL and 15.2 ng/µL, respectively.

130

131 ***Immobilization of target strands and hybridization of probes***

132 Once the glass slide was functionalized, the target strands were immobilized onto the glass slide,
133 as previously described (28). First, the PDMS slab was washed with ethanol and water and dried
134 after which it was sealed onto the functionalized glass slides. Next, 1 μL of the 5' amine-labelled
135 target solutions (or 3'-amine-labeled capture strands), all of which were diluted to 25 μM using
136 1.5 M NaCl and 0.15 M $NaHCO_3$ (immobilization buffer), were injected by a pipettor into the
137 wells of the PDMS slab. Suction was applied to the wells on the opposite side of the slab to pull
138 the solution into the microchannels.

139 The targets were allowed to react and attach to the functionalized glass slide for 1 h after which
140 the solution was pumped out of the channels, followed by a wash of the channels with the
141 immobilization buffer to get rid of any excess target strands. Next, the glass slide was put into a
142 2.5 mg/mL $NaBH_4$ bath for 15 min to reduce the imine on the target strand to an amine. The
143 glass slide was then washed with 1X PBS and dried, resulting in straight lines of the target
144 strands immobilized onto the glass slide.

145 After target strand immobilization, a second PDMS slab was reversibly sealed onto the glass
146 slide so that the biotin-labelled probe solutions (EML4 or ALK) would flow perpendicular to the
147 lines of the immobilized target strands (***Fig. 1***). One μL of probe solutions (25 nM) were diluted
148 in 1X SSC (0.15 M NaCl + 0.015 M citrate), and 0.1% sodium dodecyl sulfate (SDS) to the
149 needed concentrations, and were injected into the microchannels and allowed to hybridize to the
150 immobilized target strands for 1 h. Excess solution was then removed from the channels, and the
151 channels were subsequently washed with 1X PBS. Next, 1 μL of a 50 ng/mL streptavidin-Cy5

solution was introduced into the channels and allowed to bind to the biotin label on the probes for 15 min. This was followed by a wash with Tween solution in 1X PBS. The PDMS slab was peeled off and the glass slide was now ready for fluorescence scanning.

Immobilization of capture strands and hybridization first of PCR sense strand and then of probes

Immobilization of 3'-amine-labeled capture strands and subsequent washing and reduction are similar to what are described in the preceding section for the 5'-amine-labeled target strands.

After capture strand immobilization, a second PDMS slab was reversibly sealed onto the glass slide so that the PCR products (fusion or WT) would flow perpendicular to the lines of the immobilized antisense capture strands. These capture strands captured the sense strands of the PCR products, which were diluted before each experiment to the indicated concentrations, both in hybridization buffer.

With the PDMS slab still in place, 1 μL of probe solutions (25 nM), prepared in a similar way as in the preceding section, was injected into the microchannels by a pipettor and allowed to hybridize to the captured PCR strands for 1 h. Excess solution was then removed from the channels, and the channels were subsequently washed with 1X PBS. Next, 1 μL of a 50 ng/mL streptavidin-Cy5 solution was introduced into the channels and allowed to bind to the biotin label on the probes for 15 min. This was followed by a wash with Tween solution in 1X PBS. The PDMS slab was peeled off and the glass slide was now ready for fluorescence scanning.

Fluorescence Detection

If the biotin labelled probes were able to hybridize to the complementary target strands or captured PCR sense strand, then the subsequently introduced streptavidin-Cy5 would bind to the biotin and fluorescence from the Cy5 would be detected as patches at the appropriate intersections on the glass surface. However, if hybridization did not occur there would be no fluorescence at the intersections. The image of fluorescent patches was then uploaded onto the ImageQuant software and small rectangle boxes were overlaid onto the signals of the image. The intensity of each rectangular box was then averaged to obtain the intensity of the signal.

Instruments

Fluorescence scanning was achieved using the Typhoon Trio+ variable mode imager, as previously used (29), and Biorad ChemiDoc Imager. DNA amplification was conducted on the Techne ^{3}Prime Thermocycler. Analysis of the quality and quantity of PCR products was performed on the Nanodrop 2000 spectrometer, and this provides the DNA concentrations and the 260/280 and 260/230 absorbance ratios which allows assurance that the DNA is pure.

Results and Discussion

Testing of the effectiveness of the probes

Two 5'-amine-labelled target strands were immobilized onto the functionalized glass slide and then allowed to hybridize with both the EML4 and ALK probes. Using this method, we show that detection of the presence of the 55-mer and 85-mer oligomers is successful. ***Fig. 2a*** shows

that, as expected, both the EML4 and ALK probes hybridize to the 85-mer; whereas the ALK probe, but not the EML4 probe, hybridizes with the 55-mer. This difference in probe binding is sufficient in differentiating the 55-mer from the 88-mer. However, the signal intensity generated from the ALK probe is lower. ***Fig. 2b*** shows the signal intensities of the probes that bind to the respective oligomers.

It was noticed in the hybridization experiment that the 85-mer binds a lot stronger to the EML4 probe than the ALK probe. Upon reviewing the sequence of the probe, it was determined that ALK probe 1 had no G/C clamp on the 5' and 3' ends. The probe was then modified so that it had a G nucleotide on both ends (ALK Probe 2 in *Table 1*). In ***Fig. 3a***, the intensity of ALK probe 2 is more intense than ALK probe 1 indicating that the addition of the G clamps on the ends of the probe help the ALK probe better bind to both oligomers. ***Fig. 3b***, shows the difference in intensities between ALK probes 1 and 2, with ALK probe 2 showing greater intensity. For all subsequent experiments, ALK probe 2 was used.

Detection of PCR products of the EML4-ALK fusion sequence

Detection of wildtype ALK and mutated EML4-ALK double stranded DNA, which are unlabeled, required the immobilization of the sense strands on the glass slide surface. A reasonable choice is the sequence of the forward primer (sense strand) that will certainly be captured by the antisense capture strand. This capture strand should be labelled on the 3'-end, rather than the usual 5'-end, so that the captured strand could face away from the glass surface. Once this 3'-amine-labeled capture strand was immobilized onto the glass slide, the PCR product was introduced and the antisense strand latched onto the primer (***Fig. 4***). Subsequently, the probes were introduced and allowed to bind to the PCR product.

The results are shown in ***Fig. 5a,*** which shows that the signals are high for the fusion product to bind with both the EML4 and ALK probe, but is only high for the WT product to bind with the ALK probe. Moreover, the asymmetric PCR products give higher signals than the symmetric products. To obtain a better comparison of probe binding intensities, each PCR hybridization signal was normalized to the oligomer hybridization signal within the same channel. In this way, the successful detection of the sense strand of the PCR products was defined using a signal intensity threshold normalized to the background, see ***Fig. 5b***. It shows that the fusion product binds to both the EML4 and ALK probes whereas the wildtype product binds only the ALK probe. Again, this difference in probe binding is sufficient in differentiating between the wildtype and fusion product. Since the asymmetric PCR products gave higher signals than the symmetric products, for all future experiments, it was decided that only the asymmetric PCR products would be used.

Since the ratio of mutant to wild-type DNA (i.e. mutation frequency) can vary in a given individual, a study was conducted to see how low of a mutant frequency can be detected in our biochip. Asymmetric PCR products of both fusion and WT sequences were mixed to obtain wildtype:fusion ratios of 75:25, 90:10, and 99:1. All these mixtures were diluted in hybridization buffer to the same volume. The concentration of the ALK and EML4 probes was increased to 50 nM, and 0.8 μL of the PCR product solutions were introduced twice into each channel. Detection of both the fusion and WT sequences was successful with all the mixtures listed above. ***Fig. 6a*** shows that our method is capable of detecting and differentiating the fusion and wildtype PCR

products in even the 99:1 mixture, in which the amount of fusion sequence is only 1% and at a final concentration of 0.25 ng/μL. ***Fig. 6b*** shows signal intensities of the three mixtures. The star above a bar indicates that the detection threshold was met. As can be seen in the graph, successful detection and differentiation was obtained for all 3 mixtures.

Conclusion

Detection of the EML4-ALK fusion gene and differentiation between the WT and fusion sequences has been accomplished using a microfluidic biochip. First, single stranded oligomers were directly immobilized, and the probes were subsequently introduced for detection. Next, we show that adding G clamps to the end of the ALK probe can increase the binding of this probe to the target sequences. Detection and differentiation of the fusion and WT PCR products was accomplished after immobilizing the antisense strands. Our study shows the ability to detect WT and fusion products in even the 99:1 mixture, in which the concentration of the fusion asymmetric PCR product is only 0.25 ng/μL. Further studies will be conducted by extracting mRNA from cells known to contain the EML4-ALK fusion, reverse-transcribing mRNA to cDNA, and detecting them using the method described in this work.

Conflict of Interest

The authors declare that they have no conflict of interest.

Acknowledgements

This work was supported by the Natural Sciences and Engineering Research Council (NSERC) of Canada under Grant Discovery R611277. MB is thankful for his NSERC Undergraduate Student Research Award.

Author Contributions

Original idea was conceived by Li. Experiments were designed by Boparai, with input from Li and Oberc. Experiments were performed by Boparai, with technical guidance from Oberc. Manuscript was written by Boparai with support from Li and Oberc. The project was supervised by Li.

References

[1] Rebecca L. Siegel, MPH; Kimberly D. Miller, MPH; Ahmedin Jemal, DVM, PhD. Cancer Statistics, 2018. CA CANCER J CLIN 2018;68:7–30. https://doi.org/10.3322/caac.21442.

[2] Kratzke R., Franklin M.J. (2011) Lung Cancer Epidemiology. In: Schwab M. (eds) Encyclopedia of Cancer. Springer, Berlin, Heidelberg, Pages 2100-2104. https://doi.org/10.1007/978-3-642-16483-5_6893.

[3] Ken Garber; ALK, Lung Cancer, and Personalized Therapy: Portent of the Future?, *JNCI: Journal of the National Cancer Institute*, Volume 102, Issue 10, 19 May 2010, Pages 672–675. https://doi.org/10.1093/jnci/djq184.

[4] Soda M, et al. Identification of the transforming EML4-ALK fusion gene in non-small-cell lung cancer. Nature 2007;448:561–6. https://doi.org/10.1038/nature05945.

[5] Roberts PJ. Clinical use of crizotinib for the treatment of non-small cell lung cancer. *Biologics : Targets & Therapy*. 2013;7:91-101. https://doi.org/10.2147/BTT.S29026.

[6] Hiroyuki Mano, Non-solid oncogenes in solid tumors: EML4–ALK fusion genes in lung cancer. Japanese Cancer Association Cancer Sci 2008; 99: 2349–2355. https://doi.org/10.1111/j.1349-7006.2008.00972.x.

[7] Maus MKH, Stephens C, Zeger G, Grimminger PP, Huang E. Identification of Novel Variant of EML4-ALK Fusion Gene in NSCLC: Potential Benefits of the RT-PCR Method. *International Journal of Biomedical Science : IJBS*. 2012;8(1):1-6. https://www.ncbi.nlm.nih.gov/pubmed/23675251.

[8] Tianhong Li, et al. Large-Scale Screening and Molecular Characterization of EML4-ALK Fusion Variants in Archival Non–Small-Cell Lung Cancer Tumor Specimens Using Quantitative Reverse Transcription Polymerase Chain Reaction Assays, Journal of Thoracic Oncology Volume 9, Issue 1, 2014, Pages 18-25. https://doi.org/10.1097/JTO.0000000000000030.

[9] J Lin, et al. Impact of EML4-ALK Variant on Resistance Mechanisms and Clinical Outcomes in ALK-Positive Lung Cancer, Journal of Clinical Oncology, 2018 Apr 20;36(12):1199-1206. https://doi.org 10.1200/JCO.2017.76.2294.

[10] Sabir SR, Yeoh S, Jackson G, Bayliss R. EML4-ALK Variants: Biological and Molecular Properties, and the Implications for Patients. Lai R, ed. *Cancers*. 2017;9(9):118. https://doi.org/10.3390/cancers9090118.

[11] Wen M, Wang X, Sun Y, et al. Detection of *EML4-ALK* fusion gene and features associated with *EGFR* mutations in Chinese patients with non-small-cell lung cancer. *OncoTargets and therapy*. 2016;9:1989-1995. https://dx.doi.org/10.2147%2FOTT.S100303.

[12] Yu H, Chang J, Liu F, et al. Detection of *ALK* rearrangements in lung cancer patients using a homebrew PCR assay. *Oncotarget*. 2017;8(5):7722-7728. https://doi.org/10.18632/oncotarget.13886.

[13] Eva Lin, et al., Exon Array Profiling Detects EML4-ALK Fusion in Breast, Colorectal, and Non–Small Cell Lung Cancers, Mol Cancer Res September 1 2009 (7) (9) 1466-1476. https://doi.org/10.1158/1541-7786.MCR-08-0522

[14] Kodama, Tatsushi et al., A Novel Mechanism of EML4-ALK Rearrangement Mediated by Chromothripsis in a Patient-Derived Cell Line, Journal of Thoracic Oncology , Volume 9 , Issue 11, 1638 – 1646. https://doi.org/10.1097/JTO.0000000000000311

[15] Jaksik R, Iwanaszko M, Rzeszowska-Wolny J, Kimmel M. Microarray experiments and factors which affect their reliability. Biology Direct. 2015;10:46. https://doi.org/10.1186/s13062-015-0077-2.

[16] Li, Yulong et al. Reliability Assurance of Detection of EML4-ALK Rearrangement in Non–Small Cell Lung Cancer: The Results of Proficiency Testing in China, Journal of Thoracic Oncology , Volume 11 , Issue 6 , 924 – 929. https://doi.org/10.1016/j.jtho.2016.03.004.

[17] Liu L, Zhan P, Zhou X, Song Y, Zhou X, Yu L, et al. (2015) Detection of EML4-ALK in Lung Adenocarcinoma Using Pleural Effusion with FISH, IHC, and RT-PCR Methods. PLoS ONE 10(3). https://doi.org/10.1371/journal.pone.0117032.

[18] Julie A. Vendrell et al., Detection of known and novel ALK fusion transcripts in lung cancer patients using next-generation sequencing approaches, *Scientific Reports* volume 7, Article number: 12510(2017). https://doi.org/10.1038/s41598-017-12679-8.

[19] Zhang X, Zhang S, Yang X, et al. Fusion of EML4 and ALK is associated with development of lung adenocarcinomas lacking EGFR and KRAS mutations and is correlated with ALK expression. Molecular Cancer. 2010;9:188. https://doi.org/10.1186/1476-4598-9-188.

[20] Abootaleb Sedighi and Paul C.H. Li. Kras Gene codon 12 mutation detection enabled by Gold Nanoparticles conducted in a NanoBioArray chip. Anal. Biochem. 2014, 448, 58-64. https://doi.org/10.1016/j.ab.2013.11.019.

[21] Abootaleb Sedighi, Vicki Whitehall, Paul C.H. Li, "Enhanced destabilization of mismatched DNA using gold nanoparticles offers specificity without compromising sensitivity for nucleic acid analyses", Nano Research, 2015, 8, 3922-3933. https://doi.org/10.1007/s12274-015-0893-9.

[22] Lin Wang and Paul C.H. Li, "Gold nanoparticle-assisted single base-pair mismatch discrimination on a microfluidic microarray device", Biomicrofluidics, 4, 2010, 032209, 1-9. https://doi.org/10.1063/1.3463720.

[23] Zuker M. Mfold web server for nucleic acid folding and hybridization prediction. Nucleic Acids Research. 2003;31(13):3406-3415. https://doi.org/10.1093/nar/gkg595.

[24] Owczarzy R, Tataurov AV, Wu Y, et al. IDT SciTools: a suite for analysis and design of nucleic acid oligomers. Nucleic Acids Research. 2008;36(Web Server issue):W163-W169. https://doi.org/10.1093/nar/gkn198.

[25] SantaLucia J. A unified view of polymer, dumbbell, and oligonucleotide DNA nearest-neighbor thermodynamics. *Proc Natl Acad Sci U S A*. 1998;95(4):1460-5. https://doi.org/10.1073/pnas.95.4.1460.

[26] Richard Owczarzy et al. Effects of Sodium Ions on DNA Duplex Oligomers: Improved Predictions of Melting Temperatures, *Biochemistry* 2004 *43* (12), 3537-3554. https://doi.org/10.1021/bi034621r.

[27] Breslauer KJ, Frank R, Blöcker H, Marky LA. Predicting DNA duplex stability from the base sequence. *Proc Natl Acad Sci U S A*. 1986;83(11):3746-50. https://doi.org/10.1073/pnas.83.11.3746.

[28] Abootaleb Sedighi, Christopher Oberc, Vicki Whitehall, Paul C.H. Li, "NanoHDA: A nanoparticle-assisted isothermal amplification technique for genotyping assays", Nano Research, 2017, 10, 12-21. https://doi.org/10.1007/s12274-016-1262-z.

[29] Wilson Chim, Abootaleb Sedighi, Christopher L. Brown, Ralph Pantophlet, Paul C.H. Li, "Effect of buffer composition on PNA-RNA hybridization studied in the microfluidic microarray chip", Can. J Chem. 2018, 96, 241-247. https://doi.org/10.1139/cjc-2017-0319.

Table 1. DNA Sequences for target strands, primers, and probes. Red represents the portions of the ALK gene in the fusion and the wildtype ALK (WT) strand; blue represents portions of the EML4 gene in the fusion strand

DNA strand	Nucleotide Sequence and Functionalization
ALK Probe 1	Biotin-5′-TGGCTTGCAGCTCCT-3′
ALK Probe 2	Biotin-5′-GGCTTGCAGCTCCTG-3′
EML4 Probe	Biotin-5′-CTCTACAGTAGTTTTGCTC C-3′
WT oligomer	NH_2-C_{12}-5′-TCTCCGGCATCATGATTGTGTACCGCCGGAAGCACCAGGAGCTGC AAGCCATGCA-3′
Fusion oligomer	NH_2-C_{12}-5′-TATG GAGCAAAACTACTGTAGAGCCCACACCTGGGAAAGGACCT AAAGTGTACCGCCGGAAGCACCAGGAGCTGCAAGCCATGCA-3′
EML4 Forward Primer	5′-TGGAGACTCAGGTGGAG-3′
WT Forward Primer	5′-TGATCCTCTCTGTGGTGAC-3′
Reverse Primer	5′-ATGGCTTGCAGCTCC-3′
Fusion strand (sense) in Amplicon	5′-TGGAGACTCA GGTGGAGTCA TGCTTATATG GAGCAAAACT ACTGTAGAGC CCACACCTGG GAAAGGACCT AAAGTGTACCG CCGGAAGCAC CAGGAGCTGC AAGCCAT-3′
WT strand (sense) in Amplicon	5′-TGATCCTC TCTGTGGTGA CCTCTGCCCT CGTGGCCGCC CTGGTCCTGG CTTTCTCCGG CATCATGATT GTGTACCGCC GGAAGCACCA GGAGCTGCAA GCCAT-3′
Fusion Capture strand	5′-CTCCACCTGAGTCTCCA-3′-C_6-NH_2
WT Capture strand	5′-GTCACCACAGAGAGGATCA-3′-C_6-NH_2

Fig. 1 Flow scheme of the hybridization experiments. One PDMS slab consisting of microchannels with wells on either ends of them. The slab is sealed with a glass slide and then solutions are injected into the channels. As the solution rests inside the capillaries, it interacts with the glass slide. Samples containing the target sequences are injected into the channels and allowed to interact and immobilize to the glass slide. Removal of the slab allowed the covalently-immobilized target sequences on the glass slides to be exposed for subsequent reaction (red lines). Another PDMS slab is sealed perpendicular to the immobilized target sequences on the glass slide. Biotin-labelled probe solutions (green) are injected into the channels and allows to hybridize with the immobilized target strands (red). The dots show fluorescent signals which indicates the sites of successful hybridization.

Fig. 2 Detection using the EML4 and ALK probes: a) Images of the binding of EML4 and ALK probes with 85-mer and 55-mer sequences. b) Signal intensities show good differentiation between the 88-mer and 55-mer sequences (error bars are standard deviation of 9 measurements).

Fig. 3 Use of ALK probe 2 enhanced hybridization intensity: a) ALK probe 2 with G clamps on either end binds better to the oligomers. b) Hybridization intensity of ALK probe 2 is greater than that of ALK probe 1 (error bars show standard deviation of 3 measurements)

Fig. 4 The 3-strand hybridization method used to obtain signals for the EML4-ALK sense PCR product strands

Fig. 5 Asymmetric vs. symmetric PCR product binding intensities. a) Successful detection is defined as a signal intensity greater than 20,000 when normalized to the background (as represented by the dotted line) and is indicated by the red star. b) PCR hybridization signals are normalized to the oligomer hybridization signals in the same channel for binding comparison. The signals are stronger for the asymmetric products than for the symmetric ones (error bars show standard deviation of 3 measurements)

Fig. 6 Detection of the fusion product among the WT one: a) Images for the detection of both the fusion and WT sequences at a 99:10 wildtype:fusion PCR product mixture. b) Signal intensity graph shows ability to detect and differentiate between fusion and WT PCR product mixtures of fusion:wildtype ratios of 75:25, 90:10, and 99:1 (error bars are standard deviation of 3 measurements)

Graphical Abstract

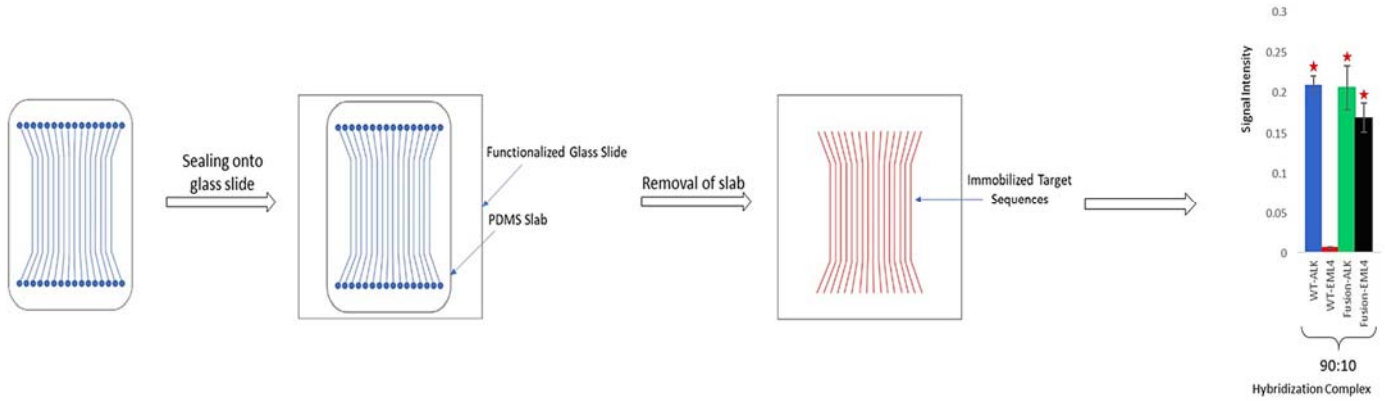

Flow scheme of the hybridization experiments performed using the microfluidic chip.